Quantitative Comparison of Classification Capability: Fully Polarimetric Versus Dual and Single-Polarization SAR

Jong-Sen Lee, *Fellow, IEEE*, Mitchell R. Grunes, *Member, IEEE*, and Eric Pottier, *Member, IEEE*

***Abstract*—This paper addresses the land-use classification capabilities of fully polarimetric synthetic aperture radar (SAR) versus dual-polarization and single-polarization SAR for P-, L-, and C-Band frequencies. A variety of polarization combinations will be investigated for application to crop and tree age classification. Based on the complex Wishart distribution for the covariance matrix, maximum likelihood (ML) classifiers for all polarization combinations were used to assess quantitative classification accuracy. Thus, this allows optimally selecting the frequency and the combination of polarizations for various applications.**

***Index Terms*—Radar polarimetry, synthetic aperture radar (SAR), terrain classification.**

I. Introduction

THE selection of radar frequency and polarization are two of the most important parameters in synthetic aperture radar (SAR) mission design. Of course, a multifrequency fully polarimetric SAR system is highly desirable, but the limitations of payload, data rate, budget, required resolution, area of coverage, etc. frequently prevent multifrequency fully polarimetric SAR from becoming a reality, especially in a spaceborne system. For a particular application, it is desirable to optimally select the frequency and combination of linear polarization channels if a fully polarimetric SAR system is not possible and to find out the expected loss in classification and geophysical parameter accuracy. In this paper, we quantitatively compare crop and tree classification accuracies between fully polarimetric SAR and multipolarization SAR for P-, L-, and C-Band frequencies. Using polarimetric P-, L, and C-Band data from NASA/JPL AIRSAR [1], the correct classification rates of crops and tree ages for all combinations of polarizations are compared. Additionally, to understand the importance of phase differences between polarizations, comparisons are also made between complex dual co-polarizations (HH and VV) and two intensity images without their phase difference.

The methodology introduced should have an impact on selecting the combinations of polarizations and frequency of a SAR for use in various applications. For example, the future C-Band ENVISAT ASAR [2] system will have dual-polarization and single polarization modes, and the C-Band RADARSAT-2 [3] and L-Band ALOS-PALSAR [4], in addition to a fully polarimetric SAR mode, will also have the dual and single polarization modes for wider swath selection.

To quantitatively evaluate the classification capability for various combinations of polarization, a procedure must be carefully established: 1) optimally supervised classification algorithms developed from the same concept should be used for all combinations of polarizations; 2) training sets have to be carefully selected from the available ground truth map; and 3) the classification reference map to be used for the classification evaluation must be reasonable and consistent with the ground truth map and polarimetric SAR data.

Comparison of classification accuracies between fully polarimetric, dual polarization and single polarization SAR data have been evaluated for P-Band, L-Band, and C-Band using two JPL AIRSAR data sets. Flevoland for crops and Les Landes for tree ages. The availability of these multi-frequency polarimetric SAR data enables us to quantitatively compare classification capabilities of all combinations of polarizations for three frequencies. Furthermore, we have ground truth maps for both scenes that facilitate the selections of training sets and reference maps.

II. Probability Density Functions (PDFs) for Multipolarization and Polarimetric SAR Data

A polarimetric SAR measures microwave reflectivity using quad-polarizations HH, HV, VH, and VV to form a scattering matrix [5]. For monostatic radar imaging of a reciprocal medium, the three unique elements of the scattering matrix define a complex vector

$$\boldsymbol{h} = [\, \boldsymbol{S}_{HH} \quad \sqrt{2}\boldsymbol{S}_{HV} \quad \boldsymbol{S}_{VV} \,]^{\,T} \tag{1}$$

where the superscript T denotes the matrix transpose. The $\sqrt{2}$ on the $\boldsymbol{S}_{HV}$ term is to ensure consistency in the span (total power) computation (see Boerner *et al.* [5]). Most SAR data are multilook processed for data volume compression and speckle reduction. The data are represented by a polarimetric covariance matrix. See (2), shown at the bottom of the page, where

superscript $*$	complex conjugate;
$\boldsymbol{n}$	number of looks;
$< \boldsymbol{S} >$	average of $\boldsymbol{S}$ over $\boldsymbol{n}$ samples.

Manuscript received Spetember 15, 2000; revised August 11, 2001. This work was supported by the Office of Naval Research under 6.1 funding, and also by ONR/NICOP-WIPSS.

J.-S. Lee and M. R. Grunes are with the Remote Sensing Division, Naval Research Laboratory, Washington DC 20375-5351 (e-mail: lee@ccf.nrl.navy.mil).

E. Pottier is with the Université de Rennes I, 35042 Rennes Cedex, France (e-mail: eric.pottier@univ-rennes1.fr).

Publisher Item Identifier S 0196-2892(01)09891-6.

It has been shown that the polarimetric covariance matrix has a complex multivariate Wishart distribution [6], [7]. Let $\boldsymbol{C} = E[\boldsymbol{Z}]$. The distribution of the $\boldsymbol{n}$ look $\boldsymbol{Z}$ given $\boldsymbol{C}$ is

$$\boldsymbol{p}_Z^{(n)}(Z|\boldsymbol{C}) = \frac{\boldsymbol{n}^{qn}\,|\boldsymbol{Z}|^{n-q}\exp[-\boldsymbol{n}Tr(\boldsymbol{C}^{-1}Z)]}{\boldsymbol{K}(\boldsymbol{n},\boldsymbol{q})\,|\boldsymbol{C}|^{n}} \tag{3}$$

and

$$\boldsymbol{K}(\boldsymbol{n},\boldsymbol{q}) = \pi^{(\frac{1}{2})q(q-1)}\Gamma(\boldsymbol{n})\cdots\Gamma(\boldsymbol{n}-\boldsymbol{q}+\mathbf{1})$$

where

$\boldsymbol{q}$	dimension of the vector $\boldsymbol{h}$;
$\boldsymbol{q}=3$	reciprocal case;
$\boldsymbol{q}=4$	bistatic case;
$\boldsymbol{Tr}$	trace of a matrix;
$\boldsymbol{K}(\mathrm{n},q)$	normalization factor.

These theoretical distributions have been verified using actual polarimetric SAR data [7].

The distribution functions for dual polarization can be derived from this complex Wishart distribution. For example, if only complex HH and VV are available, $\boldsymbol{q}=2$, and for single polarization $\boldsymbol{q}=1$, which reduces (3) to the Chi-square distribution with $2\boldsymbol{n}$ degree of freedom.

For the dual polarization case without phase difference information, the probability density function (PDF) has been derived [7]. Letting $\boldsymbol{R}_1 = <||\boldsymbol{S}_1||^2>$ and $\boldsymbol{R}_2 = <||\boldsymbol{S}_2||^2>$, we have

$$\begin{aligned} p(\boldsymbol{R}_1,\boldsymbol{R}_2) &= \frac{\boldsymbol{n}^{\boldsymbol{n+1}}(R_1R_2)^{\frac{(n-1)}{2}}\exp\left[-\frac{\boldsymbol{n}\left(\frac{\boldsymbol{R}_1}{\boldsymbol{C}_{11}}+\frac{\boldsymbol{R}_2}{\boldsymbol{C}_{22}}\right)}{\mathbf{1}-|\rho_c|^2}\right]}{(C_{11}C_{22})^{\frac{(n+1)}{2}}\Gamma(n)(\mathbf{1}-|\rho_c|^2)|\rho_c|^{n-1}} \\ &\quad\cdot \boldsymbol{I}_{\boldsymbol{n-1}}\left(2n\sqrt{\frac{\boldsymbol{R}_1\boldsymbol{R}_2}{\boldsymbol{C}_{11}\boldsymbol{C}_{22}}}\frac{|\rho_c|}{\mathbf{1}-|\rho_c|^2}\right) \end{aligned} \tag{4}$$

where

$\boldsymbol{I}_n()$	modified Bessel function of the nth order;
$\boldsymbol{C}_{11}$	$= \boldsymbol{E}[\boldsymbol{R}_1]$;
$\boldsymbol{C}_{22}$	$= \boldsymbol{E}[\boldsymbol{R}_2]$.

Maximum likelihood (ML) classification algorithms are developed based on these distributions.

III. Maximum Likelihood Classifier

In order to establish a firm foundation for comparison, we adopt supervised ML classification algorithms based on theoretical speckle distributions of multipolarization and polarimetric SAR data [7]. Supervised classification is used, because unsupervised classification [8]–[10] may cause clusters to drift away from the class centers given by the ground truth maps, and because classes from the ground truth may not correspond to the cluster centers derived from the unsupervised segmentation.

The ML classifier [11], [12] assigns a sample vector or matrix $\boldsymbol{k}$ to the $\boldsymbol{m}$ class, $\omega_{\boldsymbol{m}}$ if

$$\boldsymbol{P}(\omega_{\boldsymbol{m}}|k) \geq \boldsymbol{P}(\omega_{\boldsymbol{j}}|k), \text{for all } \boldsymbol{j} \neq \boldsymbol{m}. \tag{5}$$

Applying Bayes' rule

$$\boldsymbol{P}(\omega_{\boldsymbol{m}}|\boldsymbol{k}) = \frac{\boldsymbol{p}(\boldsymbol{k}|\omega_{\boldsymbol{m}})\boldsymbol{P}(\omega_{\boldsymbol{m}})}{\boldsymbol{p}(\boldsymbol{k})} \tag{6}$$

we have the vector or matrix $\boldsymbol{k}$ assigned to class $\omega_{\boldsymbol{m}}$ if

$$\boldsymbol{p}(\boldsymbol{k}|\omega_m)\boldsymbol{P}(\omega_m) > \boldsymbol{p}(\boldsymbol{k}|\omega_j)\boldsymbol{P}(\omega_j), \text{for all } j \neq \boldsymbol{m}. \tag{7}$$

$\boldsymbol{P}(\omega_{\boldsymbol{m}})$ is the *a priori* probability of class $\omega_{\boldsymbol{m}}$. In this application, the *a priori* probabilities are assumed to be equal. We shall discuss the ML classifier for fully polarimetric data first, followed by classifiers for dual and single polarization data.

A. Fully Polarimetric SAR Data Classifier

For terrain or land-use classification, a distance measure [13] was derived based on the ML classifier (7) and the complex Wishart distribution (3)

$$\boldsymbol{d}_3 = \ln|C_m| + Tr\left(\boldsymbol{C}_m^{-1}\boldsymbol{Z}\right) \tag{8}$$

where $\boldsymbol{C}_m = \boldsymbol{E}[\boldsymbol{Z}|\omega_m]$ is the mean covariance matrix for class $\omega_{\boldsymbol{m}}$. It is important to note that this distance measure is independent of the number of looks, $\boldsymbol{n}$. Consequently, it can be applied to single-look, multilook, and polarimetric speckle-filtered complex data. For supervised classification, training sets are required to estimate $\boldsymbol{C}_m$ for each class. The distance measure is then applied to classify each pixel.

B. Multifrequency Fully Polarimetric SAR Data Classifier

Based on the assumption that speckle is statistically independent between frequency bands, the distance measure (8) can be generalized for the classification using combined multifrequency polarimetric SAR data [13]

$$\boldsymbol{d}_{\boldsymbol{J}} = \sum_{\boldsymbol{j}=\mathbf{1}}^{\boldsymbol{J}}\left\{\ln|\boldsymbol{C}_{\boldsymbol{m}}(\boldsymbol{j})| + \boldsymbol{Tr}\left(\boldsymbol{C}_{\boldsymbol{m}}(\boldsymbol{j})^{-1}\boldsymbol{Z}(\boldsymbol{j})\right)\right\} \tag{9}$$

where

$\boldsymbol{J}$	total number of bands;
$\boldsymbol{Z}(j)$	covariance matrix for the $\boldsymbol{j}^{th}$ frequency band;
$\boldsymbol{C}_m(j)$	$= \boldsymbol{E}[\boldsymbol{Z}(\boldsymbol{j})\|\omega_{\boldsymbol{m}}]$

$$Z = \frac{\mathbf{1}}{\boldsymbol{n}}\sum_{k=1}^{n}\boldsymbol{h}(\boldsymbol{k})\boldsymbol{h}(\boldsymbol{k})^{*T} = \begin{bmatrix} <|\boldsymbol{S}_{HH}|^2> & <\sqrt{\mathbf{2}}\boldsymbol{S}_{HH}\boldsymbol{S}_{HV}^*> & <\boldsymbol{S}_{HH}\boldsymbol{S}_{VV}^*> \\ <\sqrt{\mathbf{2}}\boldsymbol{S}_{HV}\boldsymbol{S}_{HH}^*> & <\mathbf{2}|\boldsymbol{S}_{HV}|^2> & <\sqrt{\mathbf{2}}\boldsymbol{S}_{HV}\boldsymbol{S}_{VV}^*> \\ <\boldsymbol{S}_{VV}\boldsymbol{S}_{HH}^*> & <\sqrt{\mathbf{2}}\boldsymbol{S}_{VV}\boldsymbol{S}_{HV}^*> & <|\boldsymbol{S}_{VV}|^2> \end{bmatrix} \tag{2}$$

C. Dual Polarization Complex SAR Data Classifier

For classification of dual polarization complex SAR data, the (1) has only two elements, e.g.

$$\boldsymbol{w}' = [\boldsymbol{S}_1 \quad \boldsymbol{S}_2]^T. \tag{10}$$

The same distance measure (8), with $\boldsymbol{C}_m$ and $\boldsymbol{Z}$ accordingly defined as 2×2 matrices, is used for ML classification [14].

D. Single Intensity SAR Data Classifier

As mentioned in Section II, the single polarization intensity SAR data can be described by the same Wishart distribution with $\boldsymbol{q} = 1$. Letting $\boldsymbol{R}_1 =< ||\boldsymbol{S}_1||^2 >$ and $\boldsymbol{C}_{11} = \boldsymbol{E}[\boldsymbol{R}_1|\omega_{\boldsymbol{m}}]$, the distance measure for the single polarization SAR data becomes

$$\boldsymbol{d}_1 = \ln \boldsymbol{C}_{11} + \frac{\boldsymbol{R}_1}{\boldsymbol{C}_{11}}. \tag{11}$$

E. Dual Intensities SAR Data Classifier

In the absence of phase difference data, the classification is based only on two intensities. The magnitude of the complex correlation coefficient $|\rho_c|$ of (4) can be derived from two intensity images [7]. It has been proved that the correlation coefficient computed from intensities equals $|\rho_c|^2$ under the assumption of Circular Gaussian distribution. For each class, $\boldsymbol{C}_{11}, \boldsymbol{C}_{22}$, and $|\rho_c|$ are computed in a training area. A distance measure can be derived from (4) in a more complex form than (8). This distance measure does not provide a computational advantage. Consequently, the ML classifier is applied directly to the PDF (4).

IV. Classification Procedure

Ground truth maps often do not show sufficient detail for a fair evaluation of classification capabilities. Training sets have to be carefully selected from the ground truth map. Pixels in training sets are then used for all supervised classifications. To evaluate classification accuracy, the training sets may be used as the reference class map, if each training set contains a sufficient number of pixels to obtain statistically significant results. Otherwise, a reference class map may be established using the classification map from combined multifrequency polarimetric SAR data. This alternative reference map will be used for the forest age classification.

The basic classification procedure is listed as follows.

1) Select training sets from a ground truth map.
2) Filter polarimetric SAR data using the polarimetric property preserving filter [15] to reduce the effect of speckle on the classification evaluation.
3) Apply ML classifiers to:
   a) combined P-, L-, and C-Band fully polarimetric data.
   b) each individual P-Band, L-Band, or C-Band fully polarimetric data.
   c) combinations of dual polarization complex data with phase differences, complex (HH, VV), (HH, HV) and (HV, VV).
   d) combinations of dual polarizations without the phase differences ($|\mathrm{HH}|^2$, $|\mathrm{VV}|^2$), ($|\mathrm{HH}|^2$, $|\mathrm{HV}|^2$), and ($|\mathrm{HV}|^2$, $|\mathrm{VV}|^2$).
   e) each individual polarization $|\mathrm{HH}|^2$, $|\mathrm{VV}|^2$, and $|\mathrm{HV}|^2$, for all three bands.
4) Compute the correct classification rates based on the reference map.

A. Remarks

A multilook polarimetric SAR image represented by a covariance matrix has nine independent variables. Fully polarimetric classification utilizes all nine variables. However, classification based on two polarizations or one polarization is performed in a subspace, which is a projection of the nine dimensional space. Classes that are separable in the original space may not be separable in the subspace. In general, the overall correct classification rate for fully polarimetric data should be higher than for partially polarimetric data. However, this may not be true for each individual class, because many classes are involved in the classification. A pixel may be closer in distance to one class for fully polarimetric SAR, but to a different class for the dual and single polarization cases. The same also applies when comparing classification results between complex dual polarizations and two intensities without phase."

V. Comparison of Crop Classification

The JPL P-, L-, and C-Band polarimetric SAR dataset of Flevoland, The Netherlands, is used for this crop classification study. The JPL scene number is Flevoland-056–1. The image has a size of 1024×750 pixels. The pixel size is 6.6 m in the slant range direction and 12.10 m in the azimuth direction. The incidence angles are 19.7° at near range and 44.1° at far range. Most crop fields to be classified are within an 18° span of incidence angles. The change in polarimetric responses by this small variation of the incidence angle does not influence classification much. Fig. 1(a) is an L-Band image with color composed by Pauli matrix representation: red for $|\mathrm{HH} - \mathrm{VV}|$, green for $|\mathrm{HV}| + |\mathrm{VH}|$, and blue for $|\mathrm{HH} + \mathrm{VV}|$. Contrasting patches of agriculture field reveal the capability of L-Band polarimetric SAR to characterize crops. C-Band and P-Band do not have as much contrast between fields as L-Band. This dataset was collected in mid-August 1989 during the MAESTRO 1 Campaign [18], [19]. Calibration to remove the cross-talk and the channel imbalance was done by JPL. This image covers a large agricultural area of flat topography and homogeneous soils. The original ground truth map is shown in Fig. 1(b). A total of 11 classes are identified, consisting of eight crop classes from stem beans to wheat, and three other classes of bare soil, water, and forest. The color coded class label is given in Fig. 1(e) .

To obtain refined training sets, the ground-truth map was modified by eliminating the roads and all border pixels. We also observed bright noisy strips in P-Band VV [shown in Fig. 1(c)] and HV images (not shown) probably due to radio frequency interference [19]. To obtain a common training set and establish a common reference map to compare classification accuracies for all three bands, we masked out pixels on and near the bright strips from the ground truth map. The refined map shown in

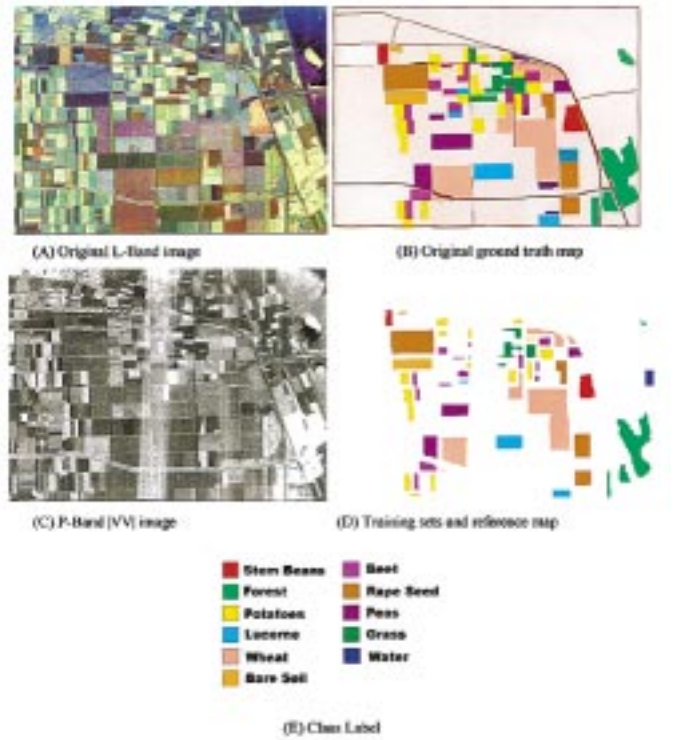

Fig. 1. L-Band polarimetric SAR image of Flevoland, The Netherlands, and its ground truth map for crop classification. (a) Original L-Band image with color composition by Pauli matrix representation: red for $|\mathrm{HH}-\mathrm{VV}|$, green for $|\mathrm{HV}|+|\mathrm{VH}|$, and blue for $|\mathrm{HH}+\mathrm{VV}|$. (b) Original ground-truth map. A total of 11 classes are identified. (c) P-Band $|\mathrm{VV}|$ image. Bright noisy strips are probably due to radio frequency interference. (d) Modified training set. (e) Color-coded class label.

Fig. 1(d) was then co-registered with SAR image and used for training and for computing classification accuracies.

The Flevoland data were originally processed with four-look average in Stokes matrix [1]. All three bands of polarimetric data were speckle filtered by applying the polarimetric property preserving filter [15] using a standard deviation to mean ratio of 0.5. The classification procedure was then applied. The correct classification rates for P-Band, L-Band, and C-Band are listed in Tables I–III, respectively. The classification results using a single polarization are shown in Table IV. Discussions on these classification results measured against the crop reference map are given in the following.

A. Fully Polarimetric Crop Classification Results

Using fully polarimetric SAR data, the classification results are shown in Fig. 2. The classes are coded with the color of Fig. 1(e). The L- Band has the best total correct classification rate of 81.65%, shown in Fig. 2(b). P-Band is the next with 71.37% shown in Fig. 2(c). C-Band is the worst with 66.53%, shown in Fig. 2(a). L-Band radar, with wavelength of 24 cm, has the proper amount of penetration power, producing better distinguished scattering characteristics between classes. C-Band does not have enough penetration, while P-Band has too much penetration. When all three bands are used for the classification, the correct classification rate increases to 91.21%, as shown in Fig. 2(d). It is apparent that multifrequency fully polarimetric SAR is highly desirable.

B. Dual Polarization Crop Classification Results

Correct classification rates for combinations of two polarization images with and without phase differences were calculated. Since correlation between co-polarization HH and VV is higher than between cross-polarization and co-polarization, we found that the phase difference between HH and VV is an important factor for crop classification. Fig. 3(a) shows L-Band classification result using the complex HH and VV. Fig. 3(b) shows the result using HH and VV intensities only. The total correct classification rate of complex HH and VV at 80.91% is only slightly inferior to that using fully polarimetric data. However, when the phase difference is not included in the classification, the rate drops to 56.35%. Phase differences are induced by differences in penetration depths between HH and VV. The difference in scattering centers between HH and VV generates important discriminating signatures shown in Fig. 3(c). Fig. 3(d) shows histograms of phase difference for each class. It reveals that all classes, except stem beans and the forest, have their phase difference highly concentrated near peaks, and most peaks do not coincide. In particular, the class of stem beans and forest have peaks located at roughly $-\pi/2$ and $\pi/4$ respectively, indicating that they are easily separated by phase differences.

The phase differences between co-polarization terms and cross-polarization terms are not as important as that between HH and VV, because co-polarization and cross-polarization terms are generally uncorrelated in distributed targets. The classification results reflect this characteristic. From Table II, the L-Band complex VV and HV with correct classification rate of 64.72% is only somewhat better than for the intensities with a rate of 60.12%.

The results of P-Band are similar except with lower overall classification rates shown in Table I. The total classification rate for complex HH and VV is 69.25%, and 59.37% for HH and VV intensities. The classification rates for the forest class for P-Band are much better than L-Band and C-Band, but P-Band is poor in separating the grass class from other crop classes. These results are expected, because P-Band has higher penetration power. The overall classification rates for C-Band are not as good, as shown in Table III. The phase difference between HH and VV is also important in C-Band classification, but the classification rate for the forest class is inferior to L-Band and P-Band, except that the grass class is better.

C. Single Polarization Data Crop Classification Results

The classification accuracies for single polarization data, as expected, are much worse than those from two polarizations. The overall correct classification rates are given in Table IV for P-, L-, and C-Band $|\mathrm{HH}|^2$, $|\mathrm{HV}|^2$ and $|\mathrm{VV}|^2$. For L-Band and C-Band, the cross polarization HV has the highest rate, but for P-Band, VV has the best rate.

D. Summary

For crop classification, it is clear that, if fully polarimetric data is not available, the combination of complex HH and VV polarizations is preferred. The contribution of co-polarization phase differences to classification is highly significant. The clas-

TABLE I
P-BAND CROP CLASSIFICATION RESULTS FOR FULLY POLARIMETRIC AND DUAL POLARIZATION DATA. THE CORRECT CLASSIFICATION RATES ARE IN PERCENTAGES. THE RESULTS FROM SINGLE POLARIZATION ARE LISTED IN TABLE IV

P-Band Crops	Fully Polarimetric	Complex HH, HV	Intensity $\|HH\|^2,\|HV\|^2$	Complex HH, VV	Intensity $\|HH\|^2,\|VV\|^2$	Complex VV, HV	Intensity $\|VV\|^2,\|HV\|^2$
Stem Bean	70.72	23.70	21.51	67.43	39.57	43.89	45.53
Forest	92.33	89.64	89.50	92.75	88.80	90.84	90.63
Potatoes	90.90	83.13	83.75	76.52	71.03	90.64	90.55
Lucerne	93.04	87.91	90.45	86.68	83.11	83.35	80.97
Wheat	54.34	30.39	28.39	53.71	37.69	43.64	36.43
Bare Soil	96.07	91.46	91.07	94.08	87.66	92.64	92.76
Beet	89.09	47.12	39.72	85.70	70.75	60.03	55.87
Rape Seed	59.13	10.80	22.85	61.60	60.27	41.22	42.80
Peas	82.04	32.98	28.24	84.69	66.17	65.63	67.07
Grass	25.01	17.77	16.19	11.35	5.59	49.77	48.95
Water	100.	86.19	86.48	100	98.51	99.43	99.36
TOTAL	71.37	46.06	46.84	69.25	59.37	61.33	59.31

TABLE II
L-BAND CROP CLASSIFICATION RESULTS FOR FULLY POLARIMETRIC AND DUAL-POLARIZATION DATA. THE CORRECT CLASSIFICATION RATES ARE IN PERCENTAGES. THE RESULTS FROM SINGLE POLARIZATION ARE LISTED IN TABLE IV

L-Band Crops	Fully Polarimetric	Complex HH, HV	Intensity $\|HH\|^2,\|HV\|^2$	Complex HH, VV	Intensity $\|HH\|^2,\|VV\|^2$	Complex VV, HV	Intensity $\|VV\|^2,\|HV\|^2$
Stem Bean	95.32	51.16	63.27	90.64	61.73	35.97	31.29
Forest	81.07	66.73	68.39	75.75	33.83	60.05	60.91
Potatoes	82.89	67.53	66.36	81.52	49.35	54.40	59.15
Lucerne	97.91	39.29	38.23	99.26	65.15	67.49	65.30
Wheat	64.80	49.77	44.27	68.02	53.72	49.43	41.65
Bare Soil	99.36	90.04	82.86	98.42	93.15	90.93	63.74
Beet	89.26	68.80	66.36	86.22	81.98	75.94	74.77
Rape Seed	89.05	55.01	53.23	87.18	49.85	82.31	77.12
Peas	86.47	50.77	39.25	84.59	65.21	81.82	79.59
Grass	91.05	66.44	65.06	90.13	71.08	75.36	75.19
Water	100	90.39	87.33	100	99.86	96.30	70.53
TOTAL	81.63	59.16	55.38	80.91	56.35	64.72	60.12

sification results using P-Band and C-Band data are inferior to those using L-Band.

E. Comparison of Tree Age Classification

For tree age classifications, we use JPL AIRSAR P-, L-, and C-Band polarimetric SAR data of Les Landes Forest, France from the MAESTRO 1 Campaign. The pixel size is 6.66 m in the slant range direction and 12.10 m in the azimuth direction. An area of 620×503 pixels containing the forested areas of the ground truth map was extract from the original image. The scene contains bare soil areas and many homogeneous forested areas of maritime pines. Six tree-age groups are included from 5-8 years to more than 41 years of age. A P-Band color composed image with red for $|HH|$, Green for $|HV|$ and blue for $|VV|$ are shown in Fig. 4(a). The available ground-truth map, courtesy of CESBIO and Dr. T. Le Toan, is shown in Fig. 4(b). A comparison of Fig. 4(a) and 4(b) reveals the backscattering coefficients increasing roughly with tree ages.

The ground-truth map is not sufficiently detailed, and inhomogeneous areas, which are revealed in polarimetric SAR images, are not shown in the map. These discrepancies forced us to select other means to create a tree class reference map for the evaluation of classification accuracy. The procedure involves careful selection of the smaller training sets shown in Fig. 4(c). It has been shown in our crop classification and by others [9] that classification based on all three bands (P-, L-, and C-Band) of polarimetric data has the highest classification rate. Consequently, the combined P-, L-, and C-Band classification map is used as the reference map for computing classification accuracies. The color coded class label is shown in Fig. 4(d).

TABLE III
C-BAND CROP CLASSIFICATION RESULTS FOR FULLY POLARIMETRIC AND DUAL POLARIZATION DATA. THE CORRECT CLASSIFICATION RATES ARE IN PERCENTAGES. THE RESULTS FROM SINGLE POLARIZATION ARE LISTED IN TABLE IV

C-Band Crops	Fully Polarimetric	Complex HH, HV	Intensity $\|HH\|^2$,$\|HV\|^2$	Complex HH, VV	Intensity $\|HH\|^2$,$\|VV\|^2$	Complex VV, HV	Intensity $\|VV\|^2$,$\|HV\|^2$
Stem Bean	66.55	24.45	12.50	57.73	22.47	53.74	55.43
Forest	46.53	36.82	37.68	43.67	35.86	34.31	26.32
Potatoes	58.09	38.18	34.16	55.28	42.02	53.60	58.73
Lucerne	92.08	83.94	84.18	81.09	75.87	89.13	88.81
Wheat	60.36	53.29	39.16	33.58	25.19	53.77	34.68
Bare Soil	95.64	95.66	95.86	95.70	90.47	95.75	96.02
Beet	48.32	48.54	50.78	48.47	42.50	27.20	24.70
Rape Seed	77.99	67.79	68.13	67.60	23.55	73.12	74.01
Peas	67.37	53.22	49.62	60.96	29.92	64.24	62.71
Grass	97.37	96.34	96.44	94.14	75.66	89.24	97.62
Water	100	100	100	100	100	100	100
TOTAL	66.53	56.39	51.54	55.00	37.22	59.72	53.72

TABLE IV
P-, L-, AND C-BAND SINGLE POLARIZATION CROP CLASSIFICATION RESULTS. THE OVERALL CORRECT CLASSIFICATION RATES ARE IN PERCENTAGES

	$\|HH\|^2$	$\|HV\|^2$	$\|VV\|^2$
P-Band	28.31	28.31	34.76
L-Band	32.49	44.81	25.74
C-Band	26.15	39.24	26.28

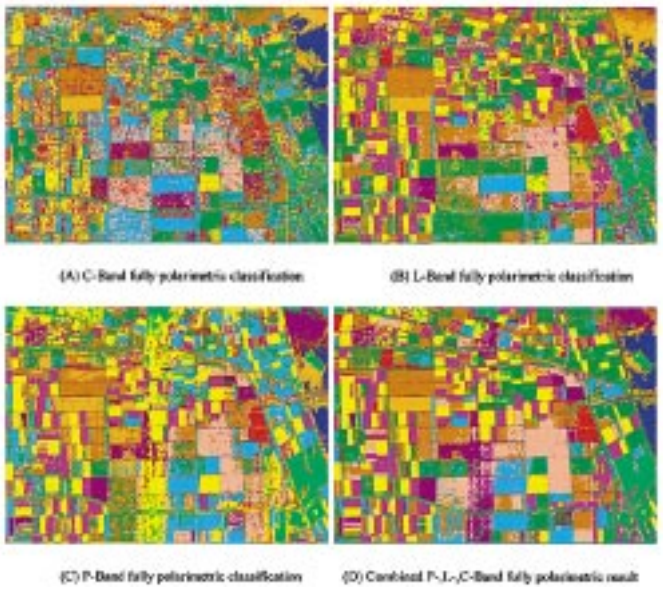

Fig. 2. Comparisons of fully polarimetric SAR crop classification results. (a) C-Band fully polarimetric classification result. The overall correct classification rate is 66.53%. (b) L-Band fully polarimetric classification result with overall rate of 81.63%. (c) P-Band fully polarimetric classification result with overall rate of 71.37%. (d) Combined P-, L-, and C-Band classification with overall rate at 91.21%.

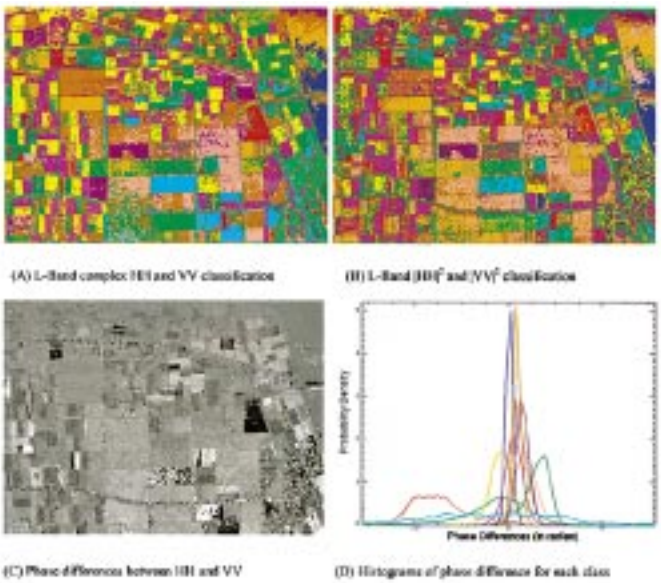

Fig. 3. Comparison of dual polarization crop classification with and without phase difference information. (a) L-Band classification results using complex HH and VV. The overall correct classification rate is 80.91%. (b) L-Band $|HH|^2$ and $|VV|^2$ (without phase difference) classification result. The overall rate drops to 56.35%. (c) The phase difference image between HH and VV displayed in gray scale between $-\pi$ and $+\pi$. (d) Histograms of phase difference for each class using the training set.

F. Fully Polarimetric Tree Age Classification Results

The classification results using fully polarimetric SAR data are shown in Fig. 5(a) for C-Band, 5(b) for L-Band, and 5(c) for P-Band. For comparison, the classification result using three bands simultaneously is shown in Fig. 5(d). Fig. 5(d) shows a good agreement with the parcel distribution given by the ground truth map of Fig. 4(b). Classification rates for each class are shown in Table V. As expected, P-Band data has much higher overall correct classification rate at 79.16% than L-Band at 64.67%. C-Band at 42.96% is not acceptable for forest classification. All three bands can separate bare soil from trees. For forest, however, the scattering mechanisms from trees are much more complex [16]. Leaves, branches, trunks and the ground create volumetric scatterings of single

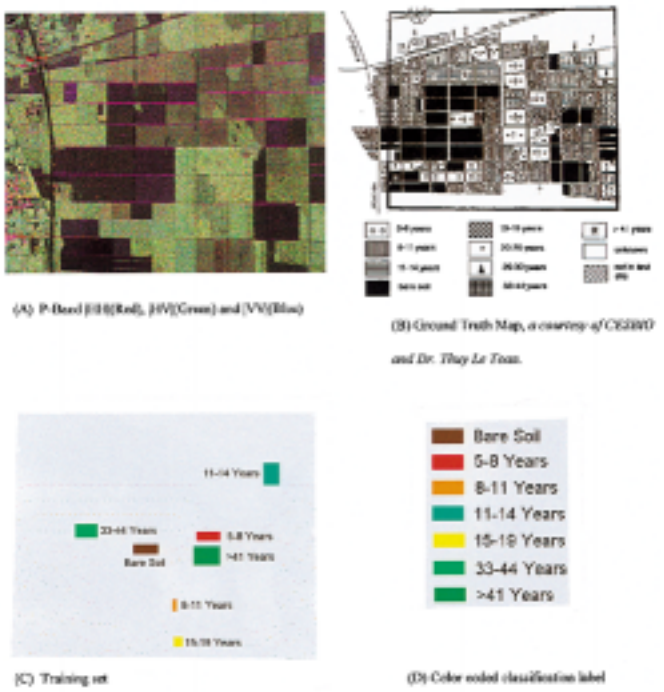

Fig. 4. P-Band polarimetric SAR image of Les Landes, France, and its ground-truth map for tree age classification. (a) Original P-Band image with color composition: red for $|\mathrm{HH}|$, green for $|\mathrm{HV}| + |\mathrm{VH}|$, and blue for $|\mathrm{VV}|$. (b) Original ground-truth map courtesy of CESBIO and Dr. T. Le Toan. A total of seven classes are identified. (c) Small training set carefully selected from the ground truth map. (d) Color-coded class label.

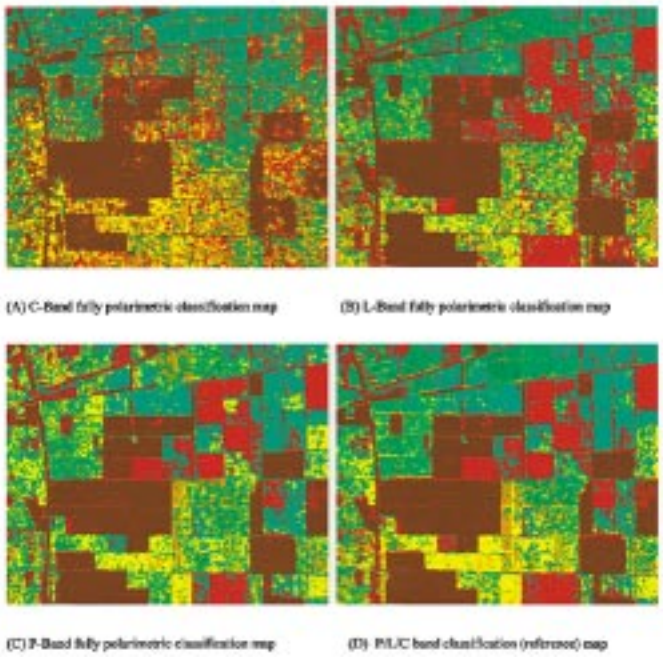

Fig. 5. Comparisons of fully polarimetric tree age classifications. (a) C-Band fully polarimetric classification result. The overall correct classification rate is 42.96%. (b) L-Band fully polarimetric classification result with the overall correct classification rate of 64.67%. (c) P-Band fully polarimetric classification result with the overall correct classification rate of 79.16%. (d) Combined P-, L-, and C-Band classification map. This map is used as reference in computing the classification accuracies for all other results.

bounce, double bounces, and multiple bounces, especially in P-Band. The L-Band has less penetration than P-Band, and its backscattered signal tends to saturate in older tree parcels. For C-Band, the dominating scattering is mainly from treetops, resulting in poor discriminating for tree ages.

G. Dual Polarization Tree Age Classification Results

For P-Band, the combination of HH and HV performs better than HH and VV as shown in Fig. 6 and Table VI. Phase differences are less influential on the classification because scattering mechanisms in tree areas are very random. Consequently, phase differences between polarizations are very noisy. The correct classification rates for P-Band are given in Table VI. The overall classification accuracy for complex HH and VV of 68.56% is very close to that for HH and VV intensities of 65.30%. This difference is much less than that from crop classification. The complex HH and HV classification accuracy is much higher at 75.95, and the HH and HV intensity classification is only slightly less at 75.44%. The difference between using and not using phases is negligible for all three dual polarization modes. We also notice that the use of HH and HV can achieve results nearly as good as that of fully polarimetric SAR. This is because of high correlation between P-Band HV polarization and tree branch biomass [20].

Classification for L-Band is similar but somewhat inferior. The performance of C-Band is much worse due to the inadequate penetration of its shorter wavelength. To save space, the C-Band and L-Band rates are not listed.

TABLE V
P-, L-, AND C-BAND TREE AGE CLASSIFICATION RESULTS FOR FULLY POLARIMETRIC DATA. THE CORRECT CLASSIFICATION RATES ARE IN PERCENTAGES

Bands / Tree Age	P-BAND Fully Polarimetric	L-BAND Fully Polarimetric	C-BAND Fully Polarimetric
Bare Soil	95.86	96.64	83.27
5-8 Years	81.72	77.52	30.51
8-11 Years	47.57	36.39	26.45
11-14 Years	86.78	49.05	33.63
15-19 Years	72.43	40.65	34.55
33-44 Years	56.64	41.73	19.57
>41 Years	57.07	56.06	21.00
TOTAL	79.16	64.67	42.96

H. Single Polarization Tree Age Classification

The overall tree age classification accuracies for single polarization are much better than those for crop classification. P-Band HV has the overall classification rate of 68.88%, HH of 58.31% and VV of 53.89%. Classification rates for single polarization are very close to those for dual polarization for all three bands. It indicates highly correlated radar returns between polarizations. Applying target decomposition of Cloude and Pottier [17] to fully polarimetric SAR images, we found that the entropies are very high for all forest areas, revealing random scattering mechanisms. In other words, the backscattered signals are very depolarized. Consequently, the polarization effect

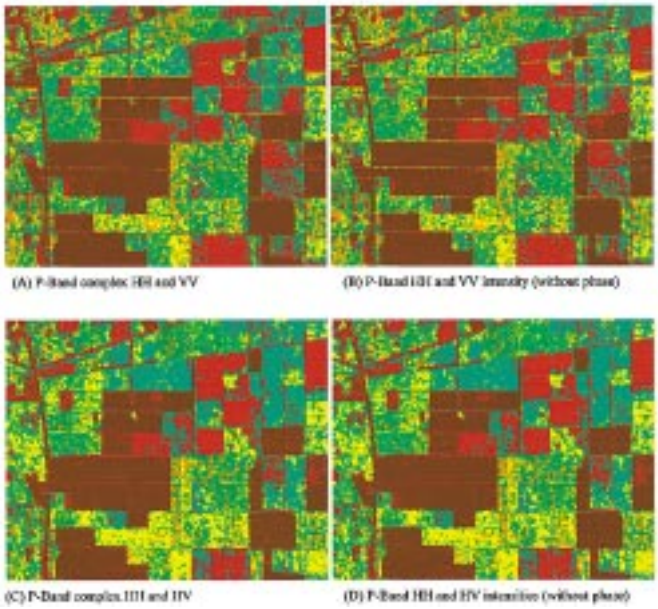

Fig. 6. Comparisons of dual polarization tree age classifications. (a) P-Band classification results using complex HH and VV. The overall correct classification rate is 68.56%. (b) P-Band $|\mathrm{HH}|^2$ and $|\mathrm{VV}|^2$ classification (without phase difference). The overall rate does not change much to 65.30%. (c) P-Band classification results using complex HH and HV. The overall correct classification rate is much higher at 75.95%. (d) P-Band $|\mathrm{HH}|^2$ and $|\mathrm{HV}|^2$ classification result with overall rate at 75.44%. These indicate that phase difference between polarizations are largely random, and do not contribute much to classification.

TABLE VI
P-BAND TREE AGE CLASSIFICATION RESULTS FOR FULLY POLARIMETRIC AND DUAL POLARIZATION DATA. THE CORRECT CLASSIFICATION RATES ARE IN PERCENTAGES

P-Band Tree Age	Complex HH, HV	Intensity $\|HH\|^2$,$\|HV\|^2$	Complex HH, VV	Intensity $\|HH\|^2$,$\|VV\|^2$	Complex VV, HV	Intensity $\|VV\|^2$,$\|HV\|^2$
Bare Soil	94.49	94.38	95.69	92.47	93.31	93.36
5-8 Years	77.58	77.31	83.51	75.46	76.85	76.60
8-11 Years	35.65	36.66	46.62	44.36	52.14	53.68
11-14 Years	80.33	79.98	61.73	57.86	87.01	86.93
15-19 Years	76.96	75.66	41.05	44.13	76.19	76.15
33-44 Years	53.93	54.74	42.92	41.92	21.36	21.79
>41 Years	49.48	44.62	53.74	49.47	25.11	20.48
TOTAL	75.95	75.44	68.56	65.30	71.64	71.37

is less significant. The reason why cross-polarization HV produces better classification results than HH and VV is because the volumetric scattering in forest areas enhances the cross-polarization returns.

VI. CONCLUSION

A procedure has been developed to quantitatively evaluate the classification capabilities for fully polarimetric combinations of dual polarization and single polarization SAR. Quantitative comparison has been made for crop and forest age classifications for P-Band, L-Band, and C-Band frequencies. The fully polarimetric and partially polarimetric classification algorithms are developed based on the principle of the ML classifier. All PDFs are derived from the complex Wishart distribution under the circular Gaussian assumption for complex polarimetric data. These optimal classifiers, developed on the same foundation, ensure a fair comparison of classification capabilities.

We found that L-Band fully polarimetric SAR data are best for crop classification, but P-Band is best for forest age classification, because longer wavelength electromagnetic waves provide higher penetration. For dual polarization classification, the HH and VV phase difference is important for crop classification but less important for tree age classification. Also, for crop classification, the L-Band complex HH and VV can achieve correct classification rates almost as good as for full polarimetric SAR data, and for forest age classification, P-Band HH and HV should be used in the absence of fully polarimetric data. In all cases, we have demonstrated that multifrequency fully polarimetric SAR is highly desirable. The methodology introduced in this paper should have an impact on the selection of polarizations and frequencies in current and future SAR systems for various applications.

ACKNOWLEDGMENT

The authors would like to thank the NASA JPL AIRSAR Team for their sustained effort in providing valuable polarimetric SAR data.

REFERENCES

[1] J. J. van Zyl and H. A. Zebker, "Imaging radar polarimetry," in *PIERS 3 Progress in Electromagnetic Research*, J.A. Kong, Ed. Amsterdam, The Netherlands: Elsevier, 1990, ch. 5.

[2] Y.-L. Desnos, H. Laur, P. Lim, P. Meisl, and T. Gach, "The ENVISAT-1 advanced synthetic aperture radar processor and data product," in *Proc. IGARSS'99*, Hamburg, Germany, July 1999.

[3] P. Meisl, A. Thompson, and A. P. Luscombe, "RADARSAT-2 Mission: Overview and development status," in *Proc. EUSAR'2000*, Honolulu, HI, May 2000, pp. 373–376.

[4] H. Wakabayashi, N. Ito, and H. Hamazaki, "PALSAR System on the ALOS," *Proc. SPIE*, pp. 181–189, 1998.

[5] W. M. Boerner *et al.*, "Polarimetry in radar remote sensing: Basic and applied concepts," in *Principles and Applications of Imaging Radar, The Manual of Remote Sensing*, 3rd ed. New York: Wiley, 1998, ch. 5.

[6] N. R. Goodman, "Statistical Analysis Based on a Certain Multi-Variate Complex Gaussian Distribution (an Introduction)," *Ann. Math. Statist.*, vol. 34, pp. 152–177, 1963.

[7] J. S. Lee, K. W. Hoppel, S. A. Mango, and A. R. Miller, "Intensity and phase statistics of multilook polarimetric and interferometric SAR imagery," *IEEE Trans. Geosci. Remote Sensing*, vol. 32, pp. 1017–1028, Sept. 1994.

[8] E. Rignot, R. Chellappa, and P. Dubois, "Unsupervised segmentation of polarimetric SAR data using the covariance matrix," *IEEE Trans. Geosci. Remote Sensing*, vol. 30, pp. 697–705, July 1992.

[9] S. R. Cloude and E. Pottier, "An entropy based classification scheme for land applications of polarimetric SAR," *IEEE Trans. Geosci. Remote Sensing*, vol. 35, pp. 68–78, Jan. 1997.

[10] J. S. Lee, M. R. Grunes, T. L. Ainsworth, L. J. Du, D. L. Schuler, and S. R. Cloude, "Unsupervised classification using polarimetric decomposition and the complex Wishart classifier," *IEEE Trans. Geosci. Remote Sensing*, vol. 37, pp. 2249–2258, Sept. 1999.

[11] J. A. Kong *et al.*, "Identification of terrain cover using the optimal terrain classifier," *J. Electronmagn. Waves Applicat.*, vol. 2, pp. 171–194, 1988.

[12] H. H. Lim *et al.*, "Classification of Earth terrain using polarimetric SAR images," *J. Geophys. Res.*, vol. 94, pp. 7049–7057, 1989.

[13] J. S. Lee, M. R. Grunes, and R. Kwok, "Classification of multi-look polarimetric SAR imagery based on complex Wishart distribution," *Int. J. Remote Sensing*, vol. 15, no. 11, pp. 2299–2311, 1994.

[14] J. S. Lee and M. R. Grunes, "Statistical analysis and segmentation of multi-look SAR imagery using partial polarimetric data," in *Proc. IGARSS'95*, Florence, Italy, 1995, pp. 1422–1424.

[15] J. S. Lee, M. R. Grunes, and G. De Grandi, "Polarmetric SAR ppeckle filtering and its implication on classification," *IEEE Trans. Geosci. Remote Sensing*, vol. 37, pp. 290–301, Mar. 1999.

[16] S. L. Durden, J. J. van Zyl, and H. A. Zebker, "Modeling and observations of the radar polarization signatures of forested areas," *IEEE Trans. Geosci. Remote Sensing*, vol. 27, pp. 2363–2373, Sept. 1999.
[17] S. R. Cloude and E. Pottier, "A review of target decomposition theorems in radar polarimetry," *IEEE Trans. Geosci. Remote Sensing*, vol. 34, pp. 498–518, Mar. 1996.
[18] P. N. Churchill and E. P. W. Attema, "The MAESTRO 1 European airborne polarimetric synthetic aperture radar campaign," *Int. J. Remote Sensing*, vol. 15, no. 14, pp. 2707–1717, 1994.
[19] G. G. Lemoine, G. F. de Grandi, and A. J. Sieber, "Polarimetric contrast classification of agricultural fields using MAESTRO 1 AIRSSAR data," *Int. J. Remote Sensing*, vol. 15, no. 14, pp. 2851–2869, 1994.
[20] A. Beaudoin, T. Le Toan, S. Goze, E. Nezry, A. Lopes, and E. Mougin, "Retrieval of forest biomass from SAR data," *Int. J. Remote Sensing*, vol. 15, no. 14, pp. 2777–2796, 1994.

Jong-Sen Lee (S'66–M'69–SM'91–F'97) received the M.A. and Ph.D. degrees from Harvard University, Cambridge, MA, in 1965 and 1969, respectively.

Since then, he has been with the U.S. Naval Research Laboratory (NRL), Washington DC, where he is presently the Head of the Image Science Section, Remote Sensing Division. He is also the Principal Investigator for several remote sensing programs on polarimetric SAR and interferometric SAR. He developed several speckle filtering algorithms that have been implemented in many GIS such as ERDAS, PCI, and ENVI. His research covers a wide spectrum of areas from control theory, operation research, and radiative transfer to SAR and polarimetric SAR image processing. He has investigated SAR image segmentation, inverse SAR, polarimetric SAR imagery statistics and speckle filtering, SAR polarimetry, and terrain/land-use classification and applications. His current research interests are in the area of SAR polarimetry, scattering signature modeling, polarimetric SAR calibration, polarimetric SAR interferometry, and unsupervised segmentation and classification using polarimetric and interferometric SAR data.

Dr. Lee has chaired and organized many sessions in international conferences. He gave tutorials at IGARSS'97 and IGARSS'98. Currently, he is an Associate Editor of IEEE TRANSACTIONS ON GEOSCIENCE AND REMOTE SENSING. He has published more than 50 papers in refereed journals and more than 100 papers in conference proceedings.

Mitchell R. Grunes (M'92) received the B.A. degree in physics from Swarthmore College, Swarthmore, PA, in 1980.

Since 1980, he has worked in the area of software development connected with data acquisition and control, computational modeling, data compression, optical and X-ray astronomy, laser, hyperspectral and radar remote sensing, image processing, noise filtering, and image segmentation and classification. He worked at the NASA Goddard Space Flight Center, Greenbelt, MD, as a Contractor with the Computer Science Corporation, then at the Department of Physics and Quantum Electronics, University of Maryland, College Park. Since 1983, he has worked at the Naval Research Laboratory, where he is currently employed by Falcon Research as a Contractor to the Remote Sensing Division. He has authored 30 research articles, and his current interests include the analysis of polarimetric and interferometric SAR data.

Eric Pottier (M'95) received the M.Sc. and Ph.D. degrees in signal processing and telecommunication from the University of Rennes 1, Rennes, France, in 1987 and 1990, respectively, and defended his Habilitation from the University of Nantes, Nantes, France, in 1998.

From 1988 to 1999, he was an Associate Professor at IRESTE-University of Nantes, where he was Head of the Polarimetry Group of the Electronic and Informatic Systems Laboratory. Since 1999, he has been a full Professor at the University of Rennes 1, where he is presently the Head of the Radar Polarimetry Group of the Antenna, Radar, and Telecommunication (ART) Laboratory. His current activities of research and education are centered in the topics of analog electronics, microwave theory, and radar imaging with emphasis in radar polarimetry. His research covers a wide spectrum of areas from radar image processing (SAR, ISAR), polarimetric scattering modeling, supervised/unsupervised polarimetric segmentation and classification to fundamentals, and basic theory of polarimetry. He is the Coordinator of the Quantitative Data Inversion Research Group of the European project Radar Polarimetry: Theory and Applications (TMR). He has supervised 25 research students to graduation (M.Sc. and Ph.D.) in radar polarimetry, covering areas from theory to remote sensing applications. He has chaired and organized 16 sessions in international conferences. He has been invited to present 19 presentations in international conferences and eleven in national conferences. He has five publications in books, 19 papers in refereed journals and more than 120 papers in conference and symposium proceedings.

Dr. Pottier was a member of the Organizing Committee of the first and second editions of the *International Workshop of Radar Polarimetry* in 1990 and 1992, the Scientific Co-Organizer (with Dr. S. R Cloude) of the third edition of this workshop in 1995, and the Scientific Chairman of the fourth edition in 1998. He was a member of the National Local Organizing Committee of the *Progress In Electromagnetic Symposium* (PIERS'98) of the Technical and Scientific Committees of European SAR 2000 (*EURSAR*) in 2000 and 2002, of the *Committee on Earth Observation Satellite SAR* (CEOS-SAR) Workshop in 1999 and 2001, and of the next Commission-F Triennium *Open Symposium on Radiowave Propagation and Remote Sensing* in 2002. He received the Best Paper Award during EUSAR2000 for his research activities, co-authored with J. S. Lee, Naval Research Laboratory, in the topic of polarimetric unsupervised segmentation of POLSAR data.